An Attitude Control System for ZA-AeroSat subject to significant Aerodynamic Disturbances

Willem H. Steyn*, Mike-Alec Kearney**

**Electrical and Electronic Engineering Department,University of Stellenbosch,
Stellenbosch, South Africa (e-mail: whsteyn@ sun.ac.za)
**Electronic Systems Laboratory, University of Stellenbosch (e-mail: mkearney@sun.ac.za)*

Abstract: This paper presents the attitude control system design of ZA-AeroSat a 2U CubeSat with four feather communication antennas also used for passive aerodynamic stabilisation. An active momentum wheel and magnetic stabilisation control system will be used to damp the aerodynamic oscillations and reduce the attitude disturbances. The satellite will form part of the QB50 constellation to gather science data in the upper layers of the troposphere in the altitude range from 350 km down to 200 km. All the satellites in the QB50 constellation will carry science payloads to be pointed to within ±10° from the velocity vector direction. At these altitudes the atmospheric density becomes significant and increases exponentially as the orbit decays rapidly over only a few months' period from launch to re-entrance in the much denser lower layers of the earth's atmosphere.

1. INTRODUCTION

QB50 is an international network of 50 CubeSats for multi-point, in-situ measurments in the lower thermosphere and re-entry research. The expected launch date is middle 2015 and South Africa's contribution to QB50 will be ZA-AeroSat, a 2U CubeSat. The satellite is a research project of the University of Stellenbosch with collaboration from the Cape Peninsula University of Technology. The main payload is a science payload supplied by the Von Karman Institute for Fluid Dynamics in Brussels, the QB50 project coordinator. The attitude control requirement for the science payload is to maintain a pointing accuracy of the sensor unit to within ±10° of the velocity vector direction and to have a pointing knowledge accuracy of within ±2°. This requirement must be met from the initial altitude of 350 km down to 200 km, in a polar circular orbit.

The main experimental purpose of ZA-AeroSat will be to demonstrate an aerodynamic stabilisation method using 4 VHF/UHF antenna feathers deployed at a 20 tilt angle from the corners of the anti-RAM spacecraft facet (see Fig.1 with body axes indicated). The mounting of the 450 x 12 x 1.5 mm feathers is done to have a minimum projected area to the "cross-wind" caused by atmospheric dragging caused by the earth's rotation and to have a maximum projected area normal to the flight direction. The latter will cause a pitch restoring torque as the satellite's centre-of-mass (CoM => close to the 2U body centre) flies ahead of the satellite's centre-of-pressure (CoP => shifted towards the feathers at the back). Due to the time varying "cross-wind" (it varies with orbit latitude and local solar time, see Fig.2), the total atmospheric pressure impact on the satellite is not aligned to the velocity direction, but causes a varying yaw attitude disturbance torque. This disturbance torque increases exponentially as the atmospheric density increases towards lower altitudes, e.g. the density at 200 km is about 35 times higher than at 350 km.
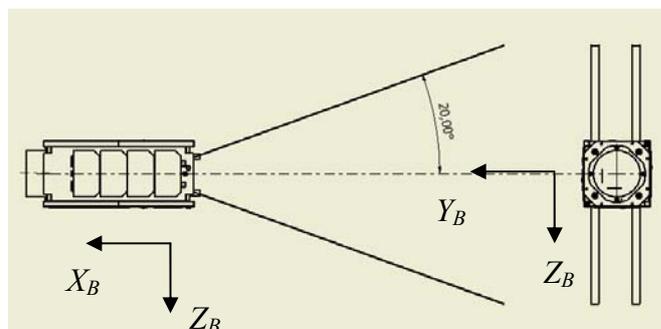
Fig. 1. Mounting of the ZA-AeroSat's feather antennas
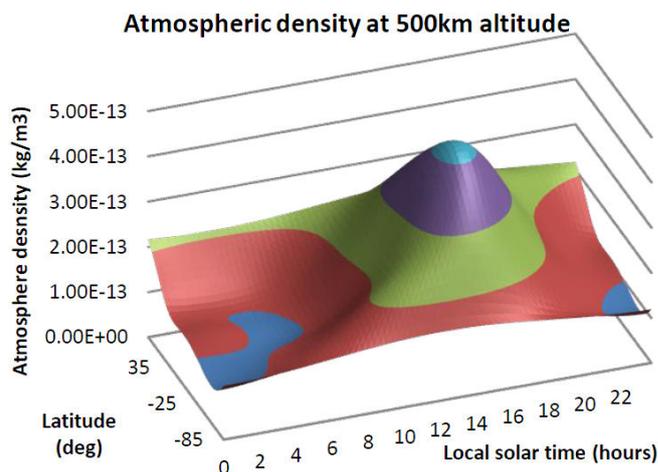
Fig. 2. Typical atmospheric density variation

The idea of using deployed feathers for passive aerodynamic and active magnetic torquing attitude stabilisation is not new (Psiaki, 2004). In this paper a finely tuned compass-like PID control law was presented to stabilise a 1U CubeSat with four deployed feathers from an altitude of 400 km polar orbit in about 10 hours, with peak pointing errors between 10° and 30°. The aerodynamic feather configuration was further

explored on a 3U CubeSat (Auret et.al. 2011), with dual control paddles to aerodynamically control the roll axis. Simulation results from a 500 km circular polar orbit show pitch, yaw pointing errors within ±10° and roll errors within ±15°, for the compass-like PID controller. If the roll control paddles are used (using a windmill configuration) in combination with a magnetic cross-product controller, the pointing errors in all axes are reduced to below ±5°. An added Y-momentum wheel to gyroscopically stiffen the roll and yaw axes and control the pitch axis, could reduce the pitch pointing error close to zero, as expected. The roll and yaw pointing errors did not reduce noticably. This result can be contributed to the "cross-wind" disturbance torque to the yaw axis now causing roll axis nutation coupling.

This paper will explore the feasibility of passive aerodynamic feather control, combined with active Y-momentum (pitch) wheel and magnetic control in the much higher atmospheric density regions at low altitude. The payload pointing requirement must be satisfied at 2 orders of magnitude higher atmospheric density and yaw disturbance torque conditions, than published previously.

2. ADCS HARDWARE DESIGN

This section presents the attitude actuators and sensors to actively control the solar sail's attitude. A summary of the important features of the attitude determination and control system (ADCS) sensors and actuators used, is listed below:

Table 1. ADCS Sensors and Actuators

Sensors & Actuators	Type	Range / FOV	Accuracy (RMS)
Magnetometer	3-axis MagR	± 60 µT	< 40 nT
Sun Sensor	2-axis CMOS	Hemisphere	< 2° peak
Nadir Sensor	2-axis CMOS	± 45°	< 2° peak
Coarse Sun	6 Photodiodes	Full Sphere	< 10°
Rate Sensor	MEMS	± 75°/sec	< 0.05 deg/sec
Momentum Pitch wheel	BDC Motor	± 2 milli-Nms	< 0.01 milli-Nms
Magnetorquers	Ferro-magnetic rods & air coil	± 0.2 Am²	< 0.0002 Am²
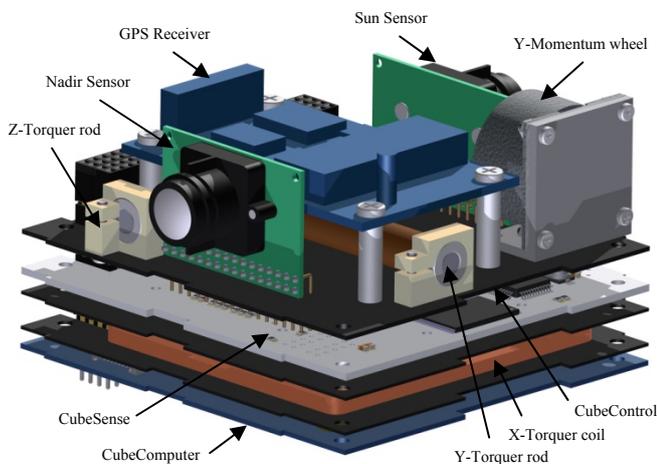
Fig. 3. ADCS Hardware bundle for ZA-AeroSat

In Fig.3 the approximate 0.5U size ADCS hardware bundle as implemented for the QB50 mission, is shown. It consists of 3 CubeSat modules: 1) *CubeComputer* an ARM Cortex based onboard computer (OBC) for implementing the satellite housekeeping and implementing the ADCS software, 2) *CubeSense* a dual sun and nadir CMOS camera based attitude sensor (see more detail below) and 3) *CubeControl* an ADCS interface unit for the magnetometer, coarse sun sensors, Y-rate sensor, magnetic torquers and the Y-momentum wheel (*CubeWheel*). A space GPS receiver is also mounted on *CubeControl*, but interfaced to the OBC to accurately determine the satellite's position for logging with the science payload data.

Magnetometer: A magneto-resistive 3-axis magnetic field sensor will be mounted on a 6 cm deployable arm (Fig.4). The deployment will take place after ejection from the QB50 launch dispenser. The sensor deployment away from the CubeSat body will reduce any magnetic contamination, caused by the onboard sub-systems. The three analogue output channels of the magnetometer are low pass filtered and A/D converted in the *CubeControl* ADCS interface unit.
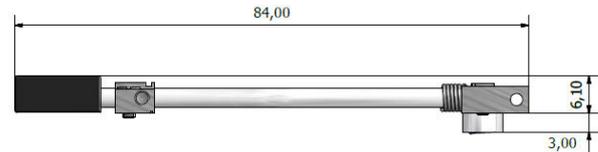
Fig. 4. Deployable Magnetometer

Sun & Nadir sensor (CubeSense): A dual camera sensor was developed for CubeSats. The sensor is based on a low power CMOS camera module of 640 by 480 pixels with a 190° field of view (FOV) fisheye lens. The one camera is used as a sun sensor with an added 0.01% neutral density filter to reduce the sun illumination levels on the camera pixels. This camera will measure the sun vector direction in a full hemisphere. The other camera will be used to measure the nadir vector by doing some signal processing on the illuminated earth disc measurement in its hemispherical FOV. The dual (sun and nadir) cameras are mounted with boresights in opposite directions, with the sun sensor in the zenith direction and the nadir sensor as the name implies. Figs. 5 and 6 show the sun and nadir vector ground calibrated measured accuracies.
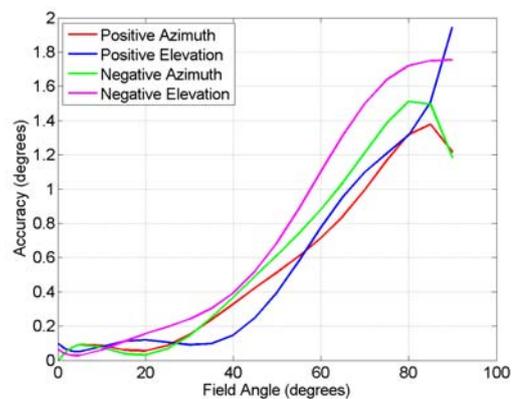
Fig. 5. Sun sensor measured accuracy
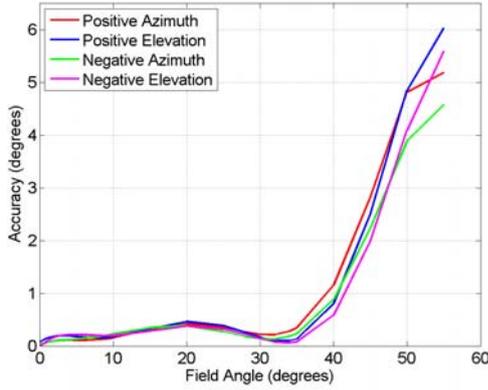
Fig. 6. Nadir sensor measured accuracy

Y-Momentum Wheel: A brushless DC motor (BDCM) driver on the *CubeControl* module will be used to accurately control the speed of a nano inertia disc mounted to a BDCM. The disc will rotate at a nominal reference speed of 4000 rpm (50% of maximum) resulting in an angular momentum vector of magnitude 0.001 Nms along the body Y_B-axis.

Magnetic Torquers: Two ferro-magnetic torquers rods (MT) (Y_B- & Z_B-axis) and an air-core coil (X_B-axis) are used to generate a controlled magnetic moment in all body axes. By pulse width modulation (PWM) of the MT currents a magnetic moment vector in a desired direction and size can be delivered. A maximum magnetic moment of 0.2 Am^2 is obtained using 2.5 V at 83 mA current (200 mW).

3. ATMOSPHERIC DISTURBANCE MODEL

The satellite orbit's position $\mathbf{u}_I$ and velocity $\mathbf{v}_I$ vectors will be modelled/measured in the J2000 earth-centered inertial (ECI) frame. To transform from the ECI frame to the orbit reference coordinate (ORC) frame, as a frame to define the satellite's attitude, the following transformation matrix can be calculated, using the unit position $\bar{\mathbf{u}}_I$ and unit velocity $\bar{\mathbf{v}}_I$ vectors:

$$\mathbf{A}_{I/O} = \begin{bmatrix} \left(\bar{\mathbf{u}}_I \times \left(\bar{\mathbf{v}}_I \times \bar{\mathbf{u}}_I\right)\right)^T \\ \left(\bar{\mathbf{v}}_I \times \bar{\mathbf{u}}_I\right)^T \\ -\bar{\mathbf{u}}_I^T \end{bmatrix} \qquad (1)$$

The satellite's attitude is then defined as the rotation from the ORC frame to the spacecraft body coordinates (SBC). This is expressed as a quaternion vector to avoid singularities as:

$$\mathbf{q}_B^O = \begin{bmatrix} q_1 & q_2 & q_3 & q_4 \end{bmatrix}^T \qquad (2)$$

The transformation matrix between the OBC and SBC frame can be calculated as:

$$\mathbf{A}_{O/B} = \begin{bmatrix} q_1^2 - q_2^2 - q_3^2 + q_4^2 & 2(q_1q_2 + q_3q_4) & 2(q_1q_3 - q_2q_4) \\ 2(q_1q_2 - q_3q_4) & -q_1^2 + q_2^2 - q_3^2 + q_4^2 & 2(q_2q_3 + q_1q_4) \\ 2(q_1q_3 + q_2q_4) & 2(q_2q_3 - q_1q_4) & -q_1^2 - q_2^2 + q_3^2 + q_4^2 \end{bmatrix}$$
$$(3)$$

When the attitude is expressed as successive Euler 2-1-3 angle rotations, the pitch θ, roll ϕ and yaw ψ rotations can be calculated as:

$$\theta = \arctan 4(A_{31}, A_{33}) \quad - \quad \{4 \text{ quadrant atan}\}$$
$$\phi = -\arcsin(A_{32}) \qquad (4)$$
$$\psi = \arctan 4(A_{12}, A_{22})$$

The dominant external disturbance torque on the satellite at low altitude, as in the case of the QB50 mission, will be aerodynamic torque disturbances caused by the atmospheric drag force on the external surfaces of the satellite. These torques can be calculated by using the panel method of partial accommodation theory. The external surface of the satellite is divided into several flat segments and the torque disturbance of each segment calculated and summed for the total disturbance torque (Steyn *et al.*, 2011):

$$\mathbf{N}_{Aero} = \sum_{i=1}^n \left\{ \begin{array}{l} \rho(\mathbf{u}_I, t) \left\|\mathbf{v}_A^B\right\|^2 A_i \cos(\alpha_i) \times \\ \left[\sigma_t\left(\mathbf{r}_i \times \bar{\mathbf{v}}_A^B\right) + \{\sigma_n S + (2 - \sigma_n - \sigma_t)\cos(\alpha_i)\}\left(\mathbf{r}_i \times \bar{\mathbf{n}}_i\right)\right] \end{array} \right\}$$

with, $\qquad (5)$

$\rho(\mathbf{u}_I, t)$ = Atmospheric density at orbit position and local time

$$\mathbf{v}_A^B = \mathbf{A}_{O/B}\mathbf{A}_{I/O}\left[\mathbf{u}_I \times \begin{bmatrix} 0 \\ 0 \\ -\omega_E \end{bmatrix}\right] - \mathbf{v}_I \qquad (6)$$

= Atmospheric velocity vector in SBC frame

ω_E = Earth's rotation rate = 7.29212 x 10^{-5} rad/s

A_i = Surface area of segment i

$\cos(\alpha_i) = \bar{\mathbf{v}}_A^B \bullet \bar{\mathbf{n}}_i$ = Cosine of angle between unit atmospheric velocity vector and $\bar{\mathbf{n}}_i$ the normal unit vector of segment i

$\mathbf{r}_i$ = Satellite CoM to segment i's CoP vector

$S = v_b / \left\|\mathbf{v}_A^B\right\|$ = Ratio of molecular exit velocity v_b to atmospheric velocity ≈ 0.1 (for 200 km to 350 km altitude)

σ_n = Normal accommodation coefficient ≈ 0.98 (for 200 km to 350 km altitude)

σ_t = Tangential accommodation coefficient ≈ 0.99 (for 200 km to 350 km altitude)

For ZA-AeroSat the 2U body panels will make a much smaller contribution to the total aerodynamic disturbance torque vector in (5), due to their smaller surface areas A_i and CoM to CoP vectors $\mathbf{r}_i$, compared to the 4 feather antennas.

4. ATTITUDE CONTROL MODES

4.1 Detumbling Mode

After release from the CubeSat launch dispenser, the satellite will be in a random body spin of less than 10 °/s in all axes. The feathers and magnetometer will then be deployed and a magnetic *Bdot* and *Y-Thompson* (Thompson, 1962) controller enabled, to dump the X_B- and Z_B-axis angular rates and to control the Y_B-axis body rate to a reference offset rate:

$$M_y = K_d \frac{d\beta}{dt} \quad \text{for} \quad \beta = \arccos\left(\frac{B_{my}}{\|\mathbf{B}_{meas}\|}\right)$$

$$M_x = K_s\left(\hat{\omega}_{yi} - \omega_{y\_ref}\right)\text{sgn}(B_{mz}) \quad \text{for} \quad |B_{mz}| > |B_{mx}| \quad (7)$$

$$M_z = -K_s\left(\hat{\omega}_{yi} - \omega_{y\_ref}\right)\text{sgn}(B_{mx}) \quad \text{for} \quad |B_{mx}| > |B_{mz}|$$

with,

β = angle between the body Y_B-axis and the magneto-meter measured B-field vector

K_d & K_s = detumbling and Y-spin controller gains

ω_{y_ref} = reference offset rate at -3 °/s

$\hat{\omega}_{yi}$ = estimated or MEMS rate sensor measured, inertial Y_B-axis body rate.

$$\mathbf{B}_{meas} = \begin{bmatrix} B_{mx} & B_{my} & B_{mz} \end{bmatrix}^T = \text{Magnetometer measurement}$$

$$\mathbf{M}_{cmd} = \begin{bmatrix} M_x & M_y & M_z \end{bmatrix}^T = \text{Commanded magnetic moment}$$

A Kalman filter rate estimator (Steyn *et al.*, 2011) can be used to estimate the satellite inertial body rates, using only the sun vector measurements during the sunlit part of the orbit. In eclipse the Kalman filter will have to propagate the body rates using a model of the satellite's dynamics. The magnetic control torque is calculated as:

$$\mathbf{N}_{MT} = \mathbf{M}_{cmd} \times \mathbf{B}_{meas} \quad (8)$$

4.2 Y-Wheel Mode

The detumbling control mode will bring the satellite to a stable Y-Thompson spin with the Y_B-axis aligned to the orbit normal direction. An Extended Kalman Filter (EKF) is then enabled to estimate the full angular state of the satellite from the magnetometer, sun and nadir vector measurements (in the SBC frame) and the corresponding modelled vectors (in the ORC frame), see (Steyn, 1995) for a detailed derivation. The 7-element discrete state vector to be estimated, is defined as:

$$\hat{\mathbf{x}}(k) = \begin{bmatrix} \hat{\boldsymbol{\omega}}_B^I(k) \\ \hat{\mathbf{q}}(k) \end{bmatrix} \quad (9)$$

with,

$$\hat{\boldsymbol{\omega}}_B^I(k) = \begin{bmatrix} \hat{\omega}_{xi}(k) & \hat{\omega}_{yi}(k) & \hat{\omega}_{zi}(k) \end{bmatrix}^T$$

the inertially referenced angular rate vector estimate, and

$$\hat{\mathbf{q}}_B^O(k) = \begin{bmatrix} \hat{q}_1(k) & \hat{q}_2(k) & \hat{q}_3(k) & \hat{q}_4(k) \end{bmatrix}^T$$

the orbit referenced quaternion vector estimate.

The orbit referenced angular rate vector estimate is then computed as:

$$\hat{\boldsymbol{\omega}}_B^O = \hat{\boldsymbol{\omega}}_B^I + \hat{\mathbf{A}}_{O/B}\begin{bmatrix} 0 & \omega_o & 0 \end{bmatrix}^T$$
$$= \begin{bmatrix} \hat{\omega}_{xo}(k) & \hat{\omega}_{yo}(k) & \hat{\omega}_{zo}(k) \end{bmatrix}^T \quad (10)$$

with,

$\omega_o = |\mathbf{v}_I|/|\mathbf{u}_I|$ = Orbit angular rate

$\hat{\mathbf{A}}_{O/B}$ = Estimated transformation matrix using $\hat{\mathbf{q}}_B^O(k)$ in (3)

The innovation used in the EKF is the vector cross-product of a measured body reference unit vector and a modelled orbit reference unit vector, transformed to the body coordinates by the estimated transformation matrix:

$$\mathbf{e}(k) = \bar{\mathbf{v}}_{meas}(k) \times \hat{\mathbf{A}}_{O/B}\,\bar{\mathbf{v}}_{model}(k) \quad (11)$$

with,

$\bar{\mathbf{v}}_{meas}$ = Magnetometer, sun, nadir sensor SBC unit vectors

$\bar{\mathbf{v}}_{model}$ = Magnetic, sun, nadir model ORC unit vectors

In this control mode the Y-momentum wheel will ensure gyroscopic stiffness to the roll and yaw axes through the Y_B direction angular momentum vector. The pitch rotation around the Y_B-axis can be controlled by implementing a quaternion feedback *Y-Wheel* PD controller (Wie *et.al.* 1989) to compute the wheel torque requirement:

$$N_{ywheel} = K_{dy}\hat{\omega}_{yo} + K_{py}\hat{q}_{2e} \quad (12)$$

with,

K_{py} & K_{dy} = proportional and derivative controller gains for optimal damping

$\hat{q}_{2e}$ = quaternion error for a desired pitch offset attitude

To prevent momentum build-up on the Y-wheel, a magnetic *Cross-Product* (13) controller (Steyn, 2010) must damp the roll and yaw gyroscopic nutation and regulate the Y-wheel angular momentum to a constant reference offset value h_{wy_ref} = -1 milli-Nms (50% of the maximum wheel momentum capacity):

$$\mathbf{M}_{cmd} = \frac{\mathbf{e} \times \mathbf{B}_{meas}}{\|\mathbf{B}_{meas}\|} \quad (13)$$

with,

$$\mathbf{e} = \begin{bmatrix} K_{dx}\hat{\omega}_{xo} + K_{px}\hat{q}_1 \\ K_{wy}\left(h_{wy} - h_{wy-ref}\right) \\ K_{dz}\hat{\omega}_{zo} + K_{pz}\hat{q}_3 \end{bmatrix} \quad (14)$$

K_{pi} & K_{di} = the proportional and derivative gains

K_{wy} = the Y-wheel momentum dumping gain

5. SIMULATION TESTS AND RESULTS

Simulation tests were done in both 350 km and 250 km circular polar orbits. The simulated initial orbit elements are presented in Table 2. All simulations were done utilising a sample period T_s = 1 sec for all models, controllers and estimators. A Simplified General Perturbations (SGP4) model was used to simulate the satellite's orbit in combination with an accurate sun orbit model. The geomagnetic field was simulated using a 10th order International Geomagnetic Reference Field (IGRF) spherical harmonic model. The satellite dynamics was simulated, using the Euler equation:

$$\mathbf{I}\dot{\boldsymbol{\omega}}_B^I = \mathbf{N}_{GG} + \mathbf{N}_{Aero} + \mathbf{N}_{MT} + \mathbf{N}_W - \boldsymbol{\omega}_B^I \times \left(\mathbf{I}\boldsymbol{\omega}_B^I + \mathbf{h}_W\right) \quad (15)$$

with,

$\mathbf{N}_{GG} = 3\omega_o^2\left(\mathbf{z}_o^B \times \mathbf{I}\,\mathbf{z}_o^B\right)$ as the gravity gradient disturbance

torque vector and $\mathbf{z}_o^B = \mathbf{A}_{O/B}\begin{bmatrix} 0 & 0 & 1 \end{bmatrix}^T$ the orbit nadir unit vector in body coordinates

$\mathbf{N}_{Aero}$ = aerodynamic disturbance torque vector calculated using the panel method from (5)

$\mathbf{N}_{MT}$ = magnetic control torque vector from (8)

$\mathbf{N}_W = \begin{bmatrix} 0 & N_{ywheel} & 0 \end{bmatrix}^T$ the Y-wheel torque from (12)

$\mathbf{h}_W = \begin{bmatrix} 0 & h_{wy} & 0 \end{bmatrix}^T$ the Y-wheel momentum

$\mathbf{I} = diag\begin{pmatrix} I_{xx} & I_{yy} & I_{zz} \end{pmatrix}$ the moment of inertia tensor, for ZA-AeroSat: $I_{xx} = 3.7 \times 10^{-3}$ kgm², $I_{yy} = 10.6 \times 10^{-3}$ kgm² and $I_{zz} = 10.3 \times 10^{-3}$ kgm²

The satellite's kinematics was simulated, using quaternions:

$$\dot{\mathbf{q}}_B^O = 0.5\,\mathbf{\Omega}\!\left(\mathbf{\omega}_B^O\right)\mathbf{q}_B^O \qquad (16)$$

with,

$$\mathbf{\Omega}\!\left(\mathbf{\omega}_B^O\right) = \begin{bmatrix} 0 & \omega_{zo} & -\omega_{yo} & \omega_{xo} \\ -\omega_{zo} & 0 & \omega_{xo} & \omega_{yo} \\ \omega_{yo} & -\omega_{xo} & 0 & \omega_{zo} \\ -\omega_{xo} & -\omega_{yo} & -\omega_{zo} & 0 \end{bmatrix}$$

Table 2. Orbit Parameters

Parameters	Orbit A	Orbit B
Perigee/Apogee	346/349 km	251/253 km
Initial inclination	97.19°	97.19°
Orbital period T_o	5488.8 sec	5371.8 sec
Eccentricity	0.000164	0.000164
LTAN	14h56	13h36
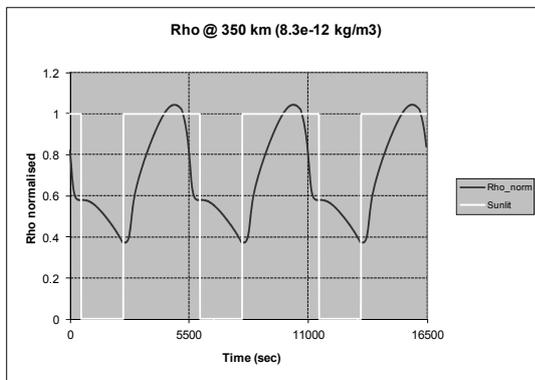
Fig. 7. Atmospheric density variation in Orbit A
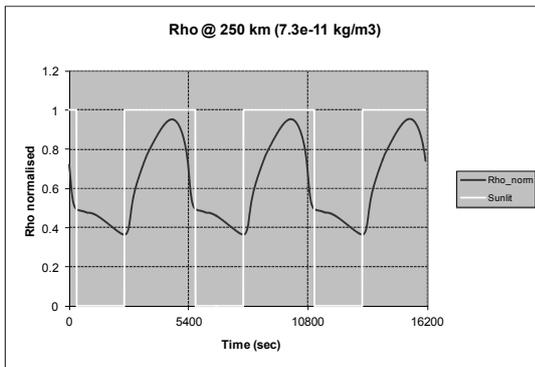
Fig. 8. Atmospheric density variation in Orbit B

Fig. 7 shows the simulated atmospheric density variation in Orbit A (normalised to the ρ_{mean} value at 350 km) and Fig. 8 for Orbit B (normalised to the ρ_{mean} value at 250km).

In Fig. 9 below the detumbling mode performance for ZA-AeroSat is presented from an initial $\mathbf{\omega}_B^O = \begin{bmatrix} 3.0 & 0.0 & -2.0 \end{bmatrix}^T$ deg/sec. For the first orbit no control is done and the *Bdot* and *Y-Thompson* controller (7) enabled at the beginning of the second orbit. It is clear that the X_B- and Z_B-axis angular rates are dumped and the Y_B-axis body rate controlled to the reference rate of -3 deg/sec within half an orbit.
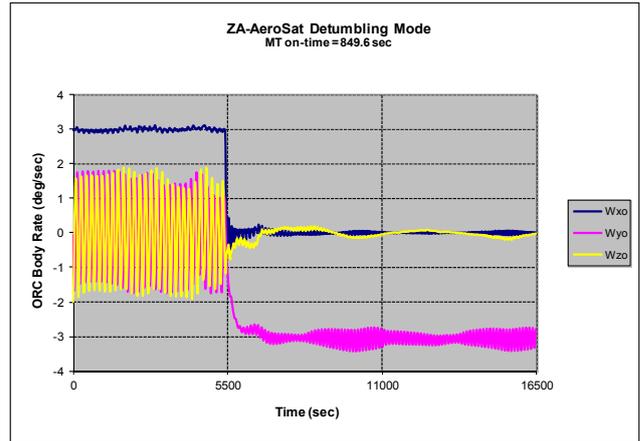
Fig. 9. ZA-AeroSat detumbling mode performance
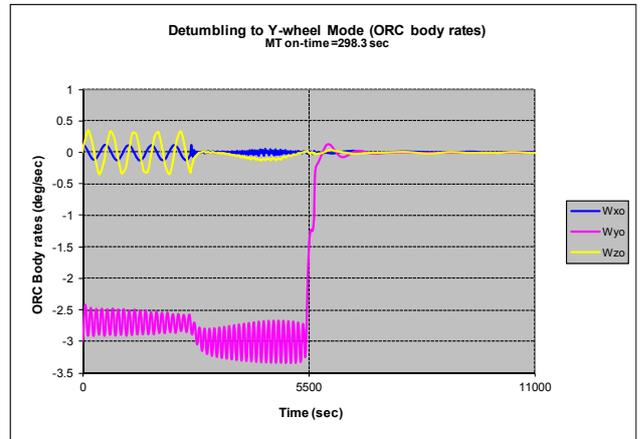
Fig.10. ZA-AeroSat detumbling to Y-Wheel mode transfer

In Fig.10 above the stable transition from the detumbling mode to the Y-Wheel mode at the end of the first orbit is shown, when the Y-momentum wheel absorbs the Y_B-axis body momentum and the *Y-Wheel* (12) and *X-Product* (13,14) controllers are enabled.

In Fig.11 the attitude performance is presented in Orbit A, from an initial pitch, roll and yaw (PRY) attitude errors of 20, -10 and 10 deg respectively. The EKF is immediately enabled and the *Y-Wheel* and *X-Product* controllers from the middle of the first orbit. The PRY attitude is eventually stabilised to maximum errors less than 2 degs in Orbit A, with the external aerodynamic disturbance torque as shown in Fig.12, satisfying the QB50 pointing specification.

In Fig.13 the attitude performance is presented in Orbit B, from similar initial pitch, roll and yaw (PRY) attitude errors

with the EKF and controllers enabled as before. The PRY attitude is eventually stabilised to maximum errors less than 4 degs in Orbit B, with the external aerodynamic disturbance torque as shown in Fig.14, again satisfying the QB50 pointing specification.
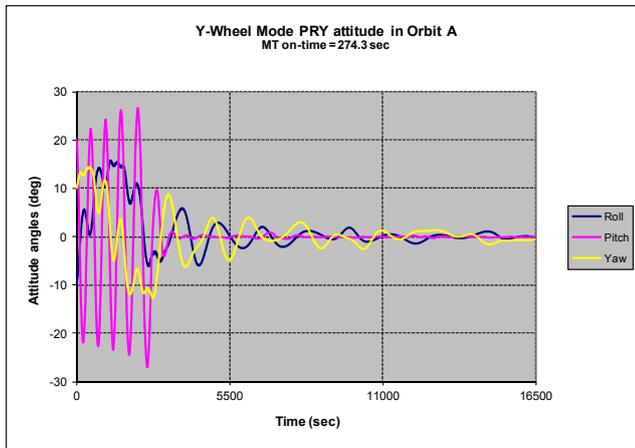
Fig.11. ZA-AeroSat Y-wheel mode attitude angles in Orbit A
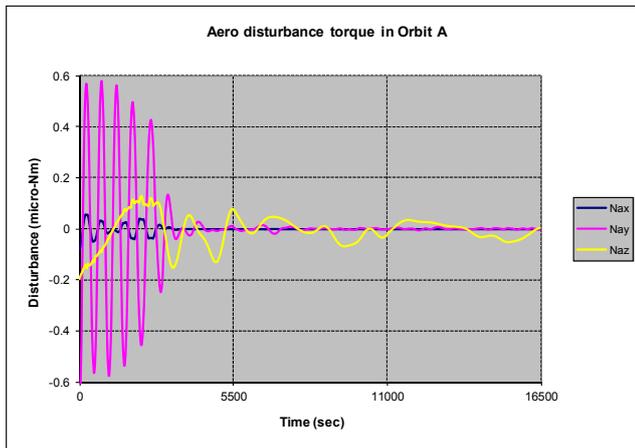
Fig.12. ZA-AeroSat aero disturbance torque in Orbit A
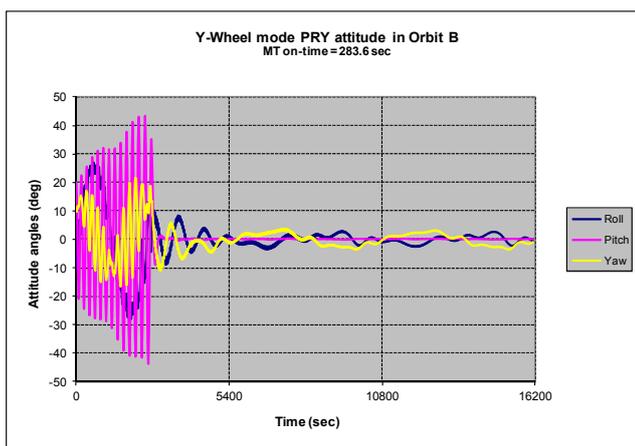
Fig.13. ZA-AeroSat Y-wheel mode attitude angles in Orbit B
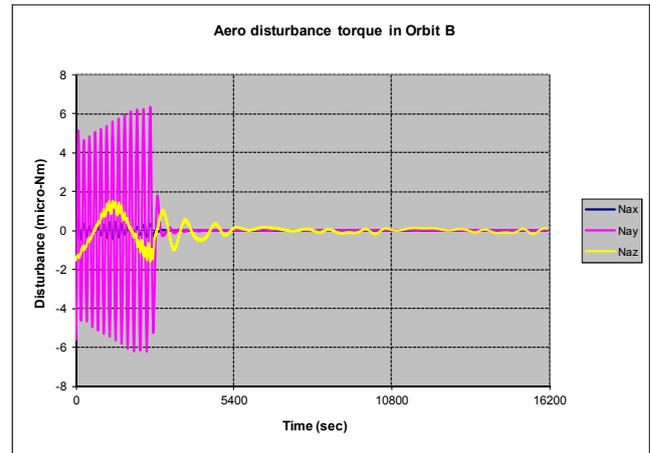
Fig.14. ZA-AeroSat aero disturbance torque in Orbit B

6. CONCLUSIONS

The attitude determination and control system design and simulation test results were presented for ZA-AeroSat. As this 2U CubeSat will be launched as a participant in the QB50 mission, it was shown that the science payload pointing requirement of within $\pm10^o$ from the velocity vector direction can easily be satisfied at 350 km and 250 km. The passive aerodynamic stabilisation method with the four feathers also combines well with the active Y-momentum wheel and 3-axis magnetic control system. The required attitude and body rate estimation with an EKF, using the magnetometer, sun and nadir vector measurements, gives estimation errors within the $\pm2^o$ pointing knowledge accuracy band specified for the science payload.

REFERENCES

Auret, J. and W.H. Steyn (2011). Design of an aerodynamic attitude control system for a CubeSat. *62th International Astronautical Congress,* Cape Town, South Africa, 3-7 Oct. IAC2011 Proceedings: **IAC-11.E2.2.3,** page 1- 9.

Psiaki, M.L. (2004). Nanosatellite attitude stabilization using passive aerodynamics and active magnetic torquing. *Journal of Guidance, Control, and Dynamics,* **Vol. 27, No. 3,** page 347 - 355.

Steyn W.H. (1995). *A Multi-Mode Attitude Determination and Control System for Small Satellites*. PhD Dissertation, University of Stellenbosch, Dec. 1995.

Steyn W.H. (2010). In-orbit AODCS performance of Sumbandilasat an earth observation satellite. *61st International Astronautical Congress*, Prague CZ, Proceedings: **IAC-10-B4.6A.4**, page 1 - 10.

Steyn W.H. & V. Lappas (2011). Cubesat solar sail 3-axis stabilization using panel translation and magnetic torquing. *Aerospace Science and Technology Journal*, **No.15**, page 476 - 485.

Thompson W.T. (1962). Spin Stabilization of attitude against gravity torque. *Journal of Astronautical Science*, **Vol. 9 No. 1,** page 31 - 33.

Wie B., H. Weiss & A. Arapostathis (1989), Quaternion Feedback Regulator for Spacecraft Eigenaxis Rotations, *AIAA Journal of Guidance, Control, and Dynamics*, **Vol.12, No.3**, page 375 - 380.